

## Optimization on springback reduction in cold stretch forming of titanium-alloy aircraft skin

HE De-hua(何德华), LI Dong-sheng(李东升), LI Xiao-qiang(李小强), JIN Chao-hai(金朝海)

School of Mechanical Engineering and Automation, Beihang University, Beijing 100191, China

Received 6 January 2010; accepted 1 July 2010

**Abstract:** An optimization method was presented for cold stretch forming of titanium-alloy aircraft skin to determine process parameters and to reduce springback. In the optimization model, a mathematical formulation of stress difference was developed as an indicator of the degree of springback instead of implicit springback analysis. Explicit finite element method (FEM) was used to analyze the forming process and to provide the stress distribution for calculating the amount of the stress indicator. In addition, multi-island genetic algorithm (MGA) was employed to seek the optimal loading condition. A case study was performed to demonstrate the potential of the suggested method. The results show that the optimization design of process parameters effectively reduces the amount of springback and improves the part shape accuracy. It provides a guideline for controlling springback in stretch forming of aircraft skin.

**Key words:** titanium alloy; aircraft skin; stretch forming; springback; optimization

### 1 Introduction

Aircraft skin is one important component comprising the aircraft aerodynamic configuration and requires high shape accuracy, which is mainly manufactured by stretch forming process in the aerospace industry[1]. Since aircraft surface is subjected to the higher and higher service temperature in modern aircrafts, especially for high speed fighters, titanium-alloy sheets have become very attractive for manufacturing aircraft skin due to their high specific strength and excellent high-temperature resistance[2–3]. For some titanium-alloy sheets with preferable formability such as TC1 and TA15, stretch forming at room temperature (also called cold stretch forming) involves a combination of elastic-plastic bending and stretch deformation. These deformations may cause a large amount of springback for the formed skin because of their higher yield strength to elastic modulus ratio[4].

Springback is a common phenomenon in sheet metal forming after removal of the sheet metal from the forming tools. Many efforts have been done to evaluate and reduce springback. Theoretical analysis is a means of interest in predicting springback, but it is difficult to get

stress fields[5–7]. Recently, FEM is widely used to evaluate the formability by explicit finite element codes and to predict springback by implicit finite element codes. Furthermore, application of optimization integrated FEM to sheet metal forming for springback reduction has attracted wide attention[8–11]. Also, ZHANG and ZHOU[12–13] introduced the same way to search for the optimal parameters for springback reduction in stretch forming of aluminium-alloy aircraft skin. Predicting the springback by implicit finite element codes is adopted in most researches. The amount of springback from the implicit springback analysis is considered the optimization objective for springback reduction. However, it is difficult to carry out the springback analysis of the aircraft skin with an implicit solving scheme, due to part of geometrical features. Also, the convergence problem often occurs in springback analysis of skins, particularly for skins of large size or complicated shape.

In this study, the optimization design was proposed to deal with cold stretch forming of titanium-alloy sheets. The measurement of springback was deduced from the forming process and the stress indicator was regarded as the objective function. Explicit FEM was used to analyze the forming process and to extract the stress for

**Foundation item:** Project(50905008) supported by the National Natural Science Foundation of China; Project(2007AA041905) supported by the National High-tech Research and Development Program of China; Project(YWF-10-01-B08) supported by the Fundamental Research Funds for the Central Universities, China

**Corresponding author:** LI Xiao-qiang; Tel: +86-10-82316584; E-mail: [littlestrong@me.buaa.edu.cn](mailto:littlestrong@me.buaa.edu.cn)  
DOI: 10.1016/S1003-6326(10)60654-1

calculating the amount of the stress indicator. Finally, a case study was carried out to demonstrate the presented optimization method.

## 2 Understanding of springback behaviour

### 2.1 Stretch wrap forming process

Stretch wrap forming process is widely used to produce skins in practice, whose basic principle is illustrated in Fig.1. First, the sheet is tensed with a force of  $F_1$  at the horizontal direction. Second, the sheet is wrapped around the die while the force  $F_1$  is kept constant and tangent to the die during the wrapping operation. Third, the final shape is formed by further stretch with a force of  $F_2$ . It is noteworthy that the sheet deformation is closely coupled with the mechanism motion. Therefore, it is a good choice to improve forming quality by adjusting loadings of mechanism motions.

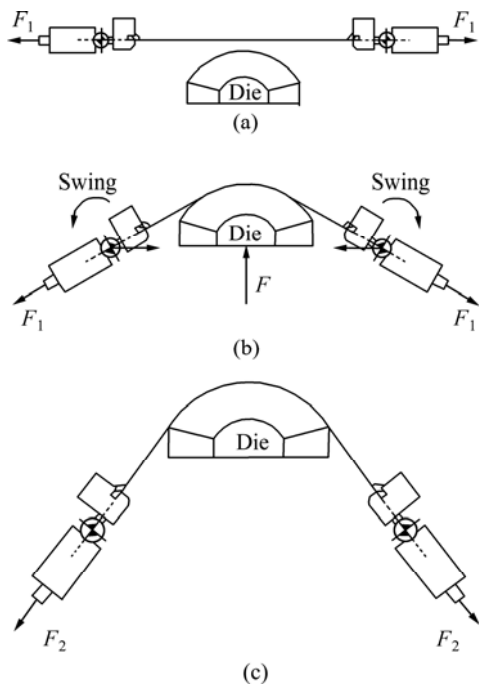


**Fig.1** Schematics of stretch wrap forming: (a) Pre-stretch; (b) Wrapping; (c) Post-stretch ( $F$ , uplift force)

### 2.2 Evolution of springback

#### 2.2.1 Basic assumptions

Fig.2 shows the geometry of the sheet metal in stretch wrap forming, whose deformation history is revealed based on the following assumptions.

1) Planes normal to the sheet surface remain plane during the deformation process.

2) The sheet is wide enough relative to its thickness. So, strain in the width direction is neglected, which means that the plane strain condition is held.

3) Normal stresses are neglected, which means that

the plane stress condition is applied.

4) Volume is conserved in the whole process.

The true strain ( $\varepsilon_b$ ) along the thickness direction owing to bending is defined as

$$\varepsilon_b = \ln \left( 1 + \frac{y}{R_0} \right) \cong \frac{y}{R_0} \quad (1)$$

where  $y$  and  $R_0$  are the distance from the mid-plane and the radius of curvature, respectively.

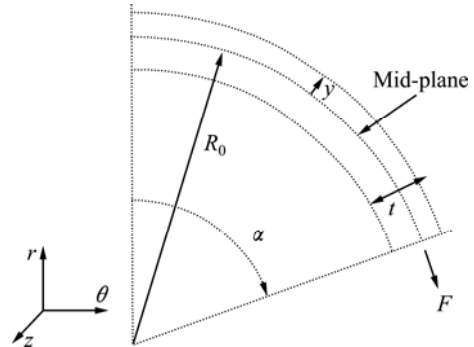


**Fig.2** Schematic view of symmetric sheet geometry under applied tensile force ( $t$ , thickness;  $F$ , applied force on sheet section;  $R_0$ , mid-plane radius of curvature;  $y$ , distance from mid-plane;  $\alpha$ , bend angle)

#### 2.2.2 Stress—strain relationships

Due to slight curvature and small thickness of aircraft skin, bending deformation is considered to be in the elastic range. For forward loading, the relationship between the stress and the strain for the material used is given by the following equation. The relationship for unloading and reverse loading will be discussed later.

$$\sigma = \begin{cases} E\varepsilon & (\varepsilon \leq \varepsilon_{e, \text{lim}}) \\ k(\varepsilon_0 + \varepsilon)^n & (\varepsilon \geq \varepsilon_{e, \text{lim}}) \end{cases} \quad (2)$$

where  $\sigma$  and  $\varepsilon$  are the effective stress and the effective strain, respectively;  $k$ ,  $n$  and  $\varepsilon_0$  are the hardening coefficient, the hardening exponent and the initial yield strain, respectively;  $E$  is the elastic modulus; and  $\varepsilon_{e, \text{lim}}$  is the elastic limit strain.

Experiments indicate that the Hill'48 quadratic yield criterion can characterize the yield behaviour of titanium-alloy sheets well[14]. According to the plastic flow principle, the Hill'48 quadratic yield criterion, assumptions (2) and (3), the following relations can be obtained:

$$\sigma = \frac{\sqrt{1+2\bar{r}}}{1+\bar{r}} |\sigma_\theta| = \frac{1}{f} |\sigma_\theta| \quad (3)$$

$$\varepsilon = \frac{1+\bar{r}}{\sqrt{1+2\bar{r}}} |\varepsilon_\theta| = f |\varepsilon_\theta| \quad (4)$$

where  $\sigma_\theta$ ,  $\varepsilon_\theta$  are the tangential stress and the tangential strain, respectively;  $\bar{r}$  is the normal

anisotropy coefficient;  $f = (1 + \bar{r}) / \sqrt{1 + 2\bar{r}}$  is a coefficient related to normal anisotropy under plane strain condition.

Fig.3 shows the development of stress and strain in the cross-section below the middle plane. The pre-stretch generally results in a deformation beyond the yield point. In the wrapping stage, the material gradually evolves from stretch to compressive deformation. Due to slight curvature and small thickness of aircraft skin, the strain  $\varepsilon_b$  caused by bending is considered to be under the elastic condition ( $|\varepsilon_b| \leq 2\sigma_{pre}/E$ ). Therefore, the reverse deformation occurs with no compressive plastic deformation. The Bauschinger effect is neglected and the isotropic hardening model is adopted. Simultaneously, the strain  $\varepsilon_w$  (the elongation of the mid-plane) caused by the constant force is taken into consideration as well. This is because upon bending the stress decreases in compression much more quickly than increases in tension, so that the part needs a deformation in order to keep the force constant. Finally, the post-stretch amount is large enough to make all deformation points go into plasticity.

Based on Eqs.(1)–(4), the tangential stress distribution throughout the sheet thickness is expressed as

$$\sigma_\theta = fk \left[ \varepsilon_0 + f \left( \varepsilon_{pre} + \frac{y}{R_0} + \varepsilon_w + \varepsilon_{post} \right) \right]^n \quad \left( -\frac{t}{2} \leq y \leq \frac{t}{2} \right) \tag{5}$$

where  $\varepsilon_{pre}$  and  $\varepsilon_{post}$  are the tangential strain of the pre-stretch and the post-stretch stages, respectively.

2.2.3 Springback measurement

In terms of the stress–strain relationship defined, the bending moment per unit width is

$$M = \int_{-t/2}^{t/2} y \sigma_\theta dy \tag{6}$$

By integration, the following equation can be obtained:

$$M = \frac{kR_0^2}{f(n+2)} \left[ \left( \varepsilon_0 + f \left( \varepsilon_{pre} + \frac{t}{2R_0} + \varepsilon_w + \varepsilon_{post} \right) \right)^{n+2} - \left( \varepsilon_0 + f \left( \varepsilon_{pre} - \frac{t}{2R_0} + \varepsilon_w + \varepsilon_{post} \right) \right)^{n+2} \right] - \frac{kR_0^2 \left[ \varepsilon_0 + f \left( \varepsilon_{pre} + \varepsilon_w + \varepsilon_{post} \right) \right]}{f(n+1)} \times \left[ \left( \varepsilon_0 + f \left( \varepsilon_{pre} + \frac{t}{2R_0} + \varepsilon_w + \varepsilon_{post} \right) \right)^{n+1} - \left( \varepsilon_0 + f \left( \varepsilon_{pre} - \frac{t}{2R_0} + \varepsilon_w + \varepsilon_{post} \right) \right)^{n+1} \right] \tag{7}$$

Note that

$$\sigma_\theta^{out} = fk \left[ \varepsilon_0 + f \left( \varepsilon_{pre} + \frac{t}{2R_0} + \varepsilon_w + \varepsilon_{post} \right) \right]^n \tag{8}$$

$$\sigma_\theta^{in} = fk \left[ \varepsilon_0 + f \left( \varepsilon_{pre} - \frac{t}{2R_0} + \varepsilon_w + \varepsilon_{post} \right) \right]^n \tag{9}$$

$$\varepsilon = f \left( \varepsilon_{pre} + \varepsilon_w + \varepsilon_{post} \right) \tag{10}$$

where  $\varepsilon$ ,  $\sigma_\theta^{out}$  and  $\sigma_\theta^{in}$  are the equivalent strain induced to the applied force, the tangential stress of the outer and the inner layer of a sheet, respectively.

By combining with Eqs.(7)–(10), the formulation of springback moment is rearranged and given by

$$M = \frac{R_0^2}{(n+2)f^{\frac{2n+2}{n}}k^{\frac{2}{n}}} \left[ \left( \sigma_\theta^{out} \right)^{\frac{n+2}{n}} - \left( \sigma_\theta^{in} \right)^{\frac{n+2}{n}} \right] - \frac{R_0^2}{(n+1)f^{\frac{2n+1}{n}}k^{\frac{1}{n}}} \left( \varepsilon_0 + \varepsilon \right) \left[ \left( \sigma_\theta^{out} \right)^{\frac{n+1}{n}} - \left( \sigma_\theta^{in} \right)^{\frac{n+1}{n}} \right] \tag{11}$$

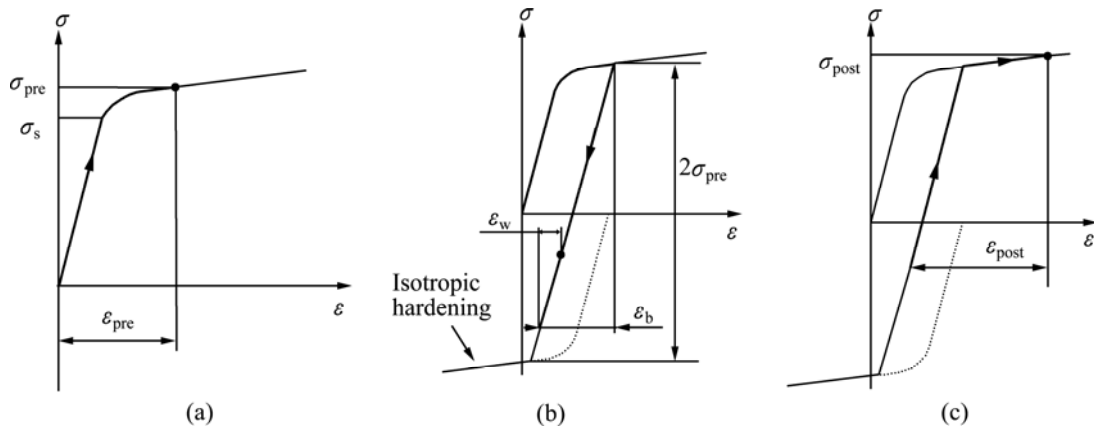


Fig. 3 Development of stress and strain for a point on inside of material: (a) Pre-stretch; (b) Wrapping; (c) Post-stretch

As known to all, springback results from the unbalanced stress throughout the thickness of a sheet. The smaller the difference of the stress throughout the thickness is, the less the springback is. Eq.(11) reveals that the springback moment depends on tangential stress state on the outer and the inner layer of the formed sheet, as well as the constant variables, including the deformation amount, the bending radius and the material properties of the formed sheet. From some research and physical considerations, the moment of the springback is directly associated with the tangential stress difference between the outer and the inner layers in stretch forming. For simplification, the springback measurement can be indicated by the following formulation:

$$f_{\text{obj}} = \sqrt{\frac{\sum_{\Omega} (\sigma_{\theta}^{\text{out}} - \sigma_{\theta}^{\text{in}})^2}{n_{\Omega}}} \quad (12)$$

where  $\Omega$ ,  $n_{\Omega}$  are the interest area on the skin part and the corresponding number of element nodes, respectively.

Eq.(12) provides an intrinsic relationship that leads to springback in stretch forming. Application of the stress indicator to springback measurement has advantages in the optimization calculation, due to its higher reliability and better usability.

### 3 Statement of optimization problem

The aim of optimization is to get the optimal process parameters which will lead to a desired part without defects, such as fracture. A conventional optimization model for sheet metal forming process can be written in the form as follows:

$$\begin{aligned} &\text{Minimize } f(X) \\ &\text{Subject to } c_i(X) \leq 0 \quad (i=1, 2, \dots, n) \end{aligned} \quad (13)$$

where  $f(X)$  and  $c_i(X)$  are the optimization objectives and the constraint conditions, respectively, with  $X$ , the design variable.

In stretch forming of titanium-alloy sheets, springback is a major problem because of their higher yield strength to elastic modulus ratio. Here, the objective function  $f(X)$  takes into account springback reduction after forming. The calculation for measuring the degree of springback combines the mathematical formulation of the stress difference with explicit FEM. Since the desired tangential stress along the thickness direction can be obtained directly from the forming simulation results, it is therefore not necessary to perform the springback analysis and to allow for the convergence problem by an implicit solving scheme[15]. The stress indicator  $f_{\text{obj}}$  is utilized as the state variable for the objective function in the optimization procedure instead of additional springback analysis.

The design variable  $X$  can be the process parameter, the material property, etc. As already illustrated in Fig.1, sheet is formed through the mechanism motions including tension cylinders and die. The loading of the mechanism motion is the most important parameter to control the material flow, which is associated with directly the part quality in the sheet forming. Therefore, the loadings of the tension cylinders are selected to be design variables, whereas the loading of the die is considered a constant value to aid the forming process.

The constraint conditions  $c_i(X)$  indicate that no defects occur during the forming, e.g. fracture. In this work, the main problem is to avoid fracture. Presently, forming limit curve (FLC) is widely applied to evaluating fracture in sheet metal forming[16], as well as the deformation amount. The constraint criterion is formulated as follows:

$$c(\varepsilon_1, \varepsilon_2) \leq 0 \quad (14)$$

$$\varepsilon \leq \varepsilon_{p, \text{lim}} \quad (15)$$

where  $c(\varepsilon_1, \varepsilon_2)$  is the forming limit curve of the formed material with  $\varepsilon_1, \varepsilon_2$ , the major strain and minor strain in the FLD, respectively;  $\varepsilon_{p, \text{lim}}$  is the limit strain for necking (Diffuse instability point). Wrinkling and severe thinning are not considered here because titanium-alloy sheet is subjected to stretch and has a good resistance to thinning due to higher normal anisotropy[17].

To find solution for the optimization problem, many algorithms have been developed, among which the multi-island genetic algorithm (MGA) exhibits great potential in nonlinear finite element analysis. MGA originated from the traditional genetic algorithm (GA), which involves a distributed GA. Fig.4 illustrates the operation description of MGA. One main feature of MGA is that the population in one generation is divided into several sub-populations termed 'islands' and all traditional genetic operations are performed separately on each sub-population. This outstanding feature not only enables the calculation to avoid converging to locally optimal solutions, but also improves the computational efficiency due to parallel

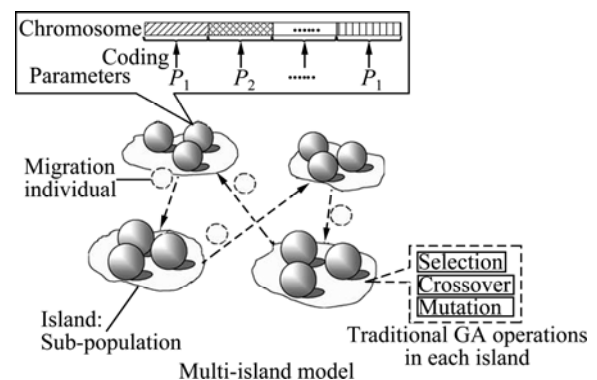


Fig.4 Schematic view of MGA operations

processing. An exchange of individual information is conducted periodically between sub-populations, called ‘migration’.

### 4 Case study

#### 4.1 Problem definition

The case discussed here concerns a double-curved aircraft skin with a radius of 500 mm in the transverse cross-section and a radius of 1 100 mm in the longitudinal cross-section, as shown in Fig.5(a). Fig.5(b) depicts the FE model based on home-made NC stretch forming machine in FE package ABAQUS. The rigid shell element was employed for stretch forming machine, while the deformable body with seven Gauss-integration points throughout thickness was adopted for the sheet.

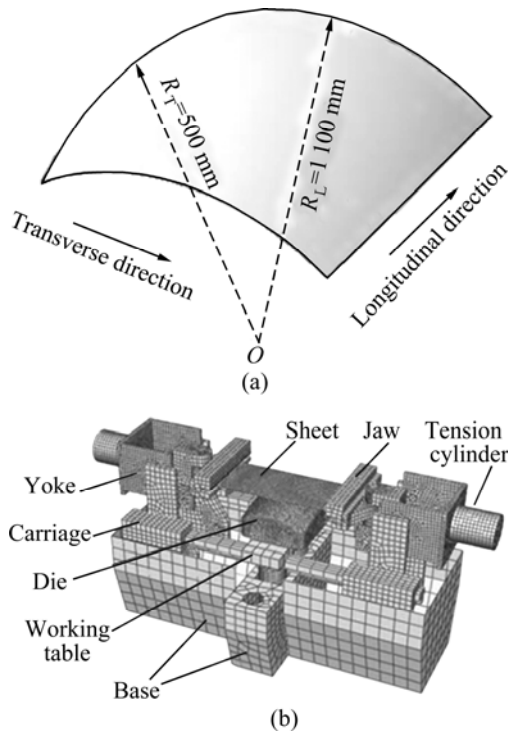


Fig.5 Geometry and FE model: (a) Part; (b) Stretch forming machine

The material model of titanium alloy TC1 used to produce this part was defined by the Hill’48 quadratic yield criterion and an isotropic hardening for plastic deformation, whose experimental strain hardening curve is illustrated in Fig.6. Other material characteristics of the sheet were given as follows: thickness,  $t_0 = 1.5$  mm; elastic modulus,  $E = 109\ 125$  MPa; Poisson ratio,  $\nu = 0.327$ ; anisotropy coefficients,  $r_0 = 1.112$ ,  $r_{45} = 2.788$ ,  $r_{90} = 3.679$ ; friction coefficient,  $\mu = 0.103$ , respectively.

According to the afore mentioned discussion, the optimization problem can be expressed as

$$\begin{aligned} & \text{Minimize} && f(X) = f_{\text{obj}} \\ & \text{Subject to} && \begin{cases} 390 \text{ kN} \leq x_{\text{pre}} \leq 430 \text{ kN} \\ 440 \text{ kN} \leq x_{\text{post}} \leq 560 \text{ kN} \\ \varepsilon_1 + 0.862\varepsilon_2 - 0.094 \leq 0 \\ \varepsilon_{\text{eqv}} \leq 0.142 \end{cases} \end{aligned} \tag{16}$$

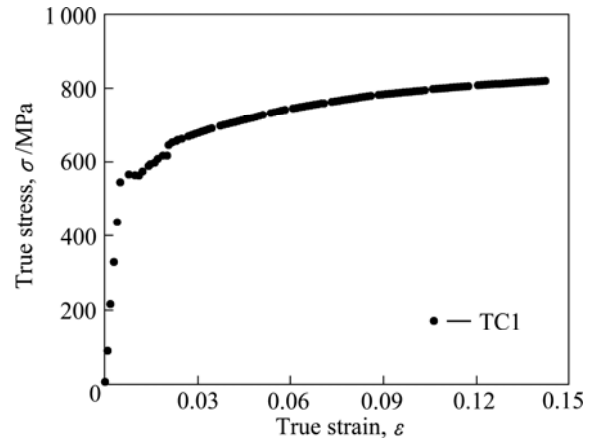
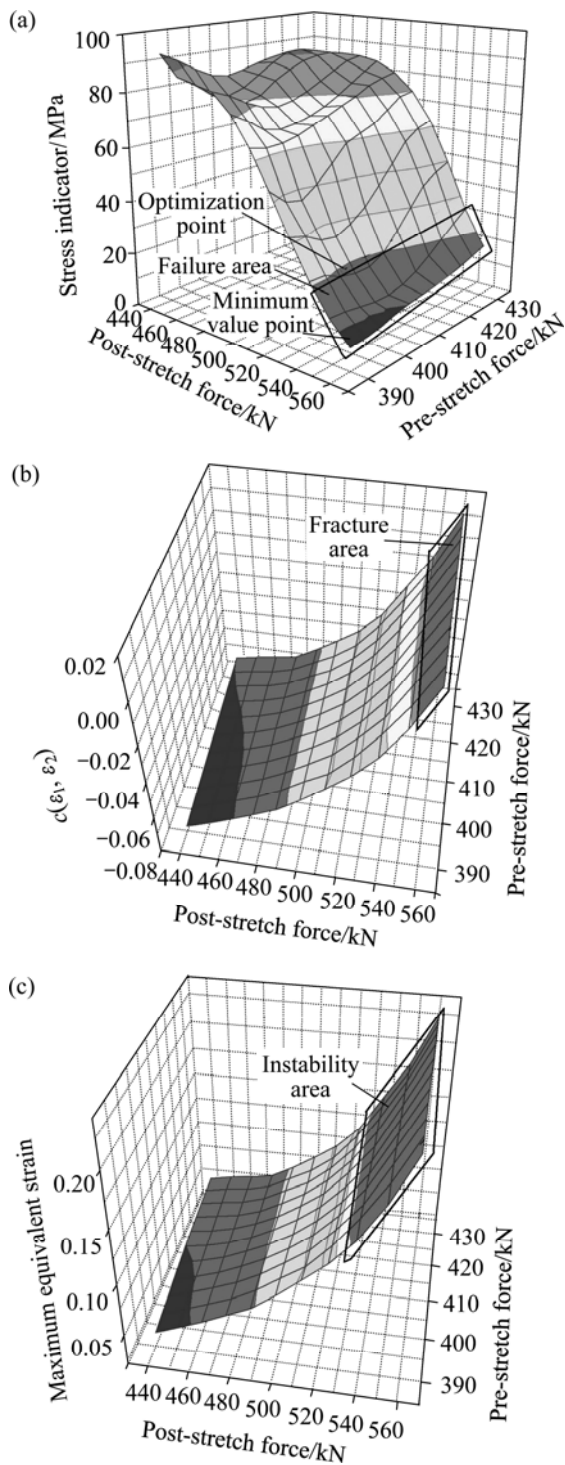


Fig.6 True stress vs true strain curve of TC1

#### 4.2 Results and discussion

By the optimization procedure with MGA, the optimal solution was achieved. Since the dominant geometry features are in the transverse direction (stretch direction), the optimal results along this direction from the sheet centre before and after optimization were mainly discussed.

Fig.7(a) represents the variation for the amount of the stress indicator with respect to the pre-stretch force and post-stretch force. The figure illustrates that the increasing pre-stretch force first leads to a slight reduction in the amount of the stress indicator, but later an increase when the pre-stretch is greater than 402.913 kN. CAO[18] delivered the similar findings before. It is thought that the higher pre-stretch beyond the initial yield point means the higher total strain when the post-stretch is added to it. However, unloading caused by bending eliminates the effect of pre-stretch below the middle plane. In view of the limited strain, the increased pre-stretch results in decreased post-stretch effect. In fact, the increasing post-stretch force can effectively reduce springback, as shown in Fig.7(a). As a whole, the amount of the stress indicator drops slightly when the post-stretch force is below 502.069 kN and decreases significantly when the post-stretch force is beyond 502.069 kN. Certainly, the larger the post-stretch force is, the smaller the springback is. But the excessive post-stretch force leads to a failure risk. Indeed, the failure occurs when the post-stretch force is more than 535.172 kN. The failure region designated in Fig.7(a) corresponds to the areas in Fig.7(b) and 7(c).



**Fig.7** Response relationship between applied force and quality factors: (a) Stress indicator; (b) Fracture; (c) Maximum equivalent strain

Furthermore, it is concluded that the applied post-stretch is more effective than the applied pre-stretch to reduce springback according to the changing magnitude of the springback amount. These results are very similar to the investigated conclusions in Refs.[19–20].

Although the minimum amount of the stress indicator is 10.596 MPa, the failure occurs

simultaneously. The available minimum amount of the stress indicator is 27.385 MPa without failure. Correspondingly, the optimal process loadings are determined as a pre-stretch force of 402.913 kN and a post-stretch force of 530.709 kN, respectively, which are listed in Table 1.

**Table 1** Comparison of optimization results

Item	Pre-stretch force/kN	Post-stretch force/kN	Stress indicator/MPa
Before optimization	420	450	82.145
After optimization	402.913	530.709	27.385

Fig.8 exhibits the tangential stress distribution of sheet transverse cross-section before and after optimization. It is clearly seen that the stress difference through the sheet thickness is large before optimization, whereas is remarkably reduced after optimization. The average stress difference of the outer and the inner layers of the sheet is up to 83.347 MPa before optimization but down to 28.272 MPa after optimization. The decrease of the stress difference means the springback reduction, as revealed in Eq.(11) and

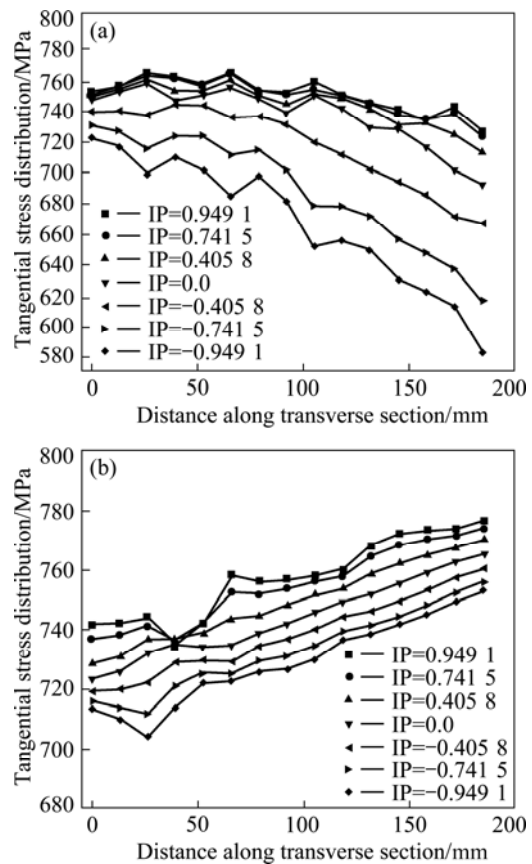


**Fig.8** Tangential stress distribution with sheet thickness integration point (IP) along sheet transverse cross-section: (a) Before optimization; (b) After optimization

other research[15]. Also, Table 1 shows that the value of the stress indicator decreases from 82.145 MPa before optimization to 27.385 MPa after optimization.

In order to demonstrate the effectiveness of this optimization method further, the springback analysis using the implicit solving scheme was implemented for comparison. Fig.9 displays the springback results, which uses the nodal displacement for springback indicator. A decrease of the springback displacement after optimization is not expected when the distance from the center is below 77.696 mm, while a significant reduction occurs when the distance is above 77.696 mm. In particular, the amount of the springback displacement corresponds well to the tangential stress distribution, as shown in Fig.8. Moreover, the maximum springback displacement decreases from 0.889 mm to 0.578 mm (see Fig.9).

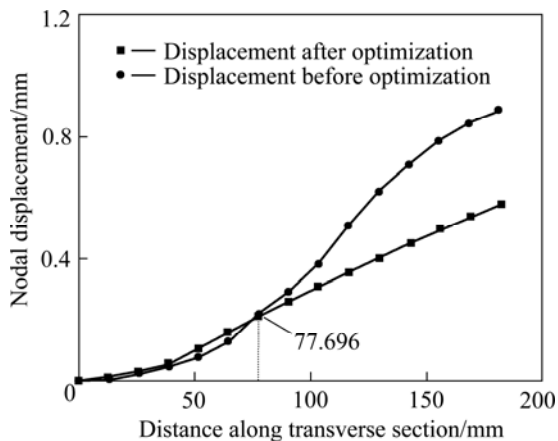


Fig.9 Springback displacements before and after optimization

Springback is a consequence of unbalanced stress throughout the thickness of a sheet experiencing bending, as previously revealed. Therefore, it is an effective method to reduce springback by decreasing the stress difference through the thickness direction. Application of the presented objective function to optimization for stretch forming of titanium-alloy sheets is demonstrated to work well for decreasing through-thickness stress difference and reducing springback.

## 5 Conclusions

1) An optimization method is presented to deal with cold stretch forming of titanium-alloy sheets. The stress indicator is considered the optimization objective, without springback simulation usually used with an implicit procedure. Explicit FEM is conducted to analyze the forming process and to obtain the stress for

calculating the amount of the stress indicator.

2) Based on stretch forming of titanium-alloy sheet, the analytical model of the springback moment is derived. This model represents well the evolution of the springback behaviour. Then the stress indicator for measuring the degree of springback is obtained from the evolution on springback.

3) The case study shows that the amount of the stress indicator decreases from 82.145 MPa before optimization to 27.385 MPa after optimization along the transverse direction, respectively. It confirms that the proposed method is feasible and efficient for springback reduction.

4) This study provides a good notion for controlling springback in sheet metal forming. Thus, it is worth developing further for process optimization of other sheet metal forming to reduce springback.

## References

- [1] ANAGNOSTOU E L. Optimized tooling design algorithm for sheet metal forming over reconfigurable compliant tooling[D]. New York: State University of New York, 2002.
- [2] SONG Hui, WANG Zhong-jin, GAO Tie-jun. Effect of high density electropulsing treatment on formability of TC4 titanium alloy sheet[J]. Transactions of Nonferrous Metals Society of China, 2007, 17(1): 87–92.
- [3] BREWER W D, KEITH BIRD R, WALLACE T A. Titanium alloys and processing for high speed aircraft[J]. Materials Science and Engineering A, 1998, 243(1): 299–304.
- [4] PALANISWAMY H, NGAILE G, ALTAN T. Optimization of blank dimensions to reduce springback in the flexforming process[J]. Journal of Materials Processing Technology, 2004, 146(1): 28–34.
- [5] ASNAFI N. On springback of double-curved autobody panels[J]. International Journal of Mechanical Science, 2001, 43(1): 5–37.
- [6] YI H K, KIM D W, VAN TYNE C J, MOON Y H. Analytical prediction of springback based on residual differential strain during sheet metal bending[J]. Journal of Mechanical Engineering Science, 2008, 222(2): 117–129.
- [7] ZHANG Dong-juan, CUI Zhen-shan, LI Yu-qiang, RUAN Xue-yu. Springback of sheet metal after plane strain stretch-bending[J]. Engineering Mechanics, 2007, 24(7): 66–71. (in Chinese)
- [8] NACEUR H, GUO Y Q, BEN-ELECHI S. Response surface methodology for design of sheet forming parameters to control springback effects[J]. Computers and Structures, 2006, 84, 1651–1663.
- [9] MEINDERS T, BURCHITZ I A, BONTE M H A, LINGBEEK R A. Numerical product design: Springback prediction, compensation and optimization[J]. International Journal of Machine Tools and Manufacture, 2008, 48(5): 499–514.
- [10] LIU Wei, YANG Yu-ying, XING Zhong-wen, ZHAO Li-hong. Springback control of sheet metal forming based on the response-surface method and multi-objective genetic algorithm[J]. Materials Science and Engineering A, 2009, 499(1/2): 325–328.
- [11] INGARAO G, DI LORENZO R, MICARI F. Analysis of stamping performances of dual phase steels: A multi-objective approach to reduce springback and thinning failure[J]. Materials and Design, 2009, 30(10): 4421–4433.

- [12] ZHANG Yan-min, ZHOU Xian-bin. Parameter optimization in aircraft skin stretch forming process[J]. *Acta Aeronautica et Astronautica Sinica*, 2006, 27(6): 1204–1208. (in Chinese)
- [13] ZHANG Yan-min, ZHOU Xian-bin. Optimization of loading trajectory for skin stretch forming process[J]. *Journal of Beijing University of Aeronautics and Astronautics*, 2007, 33(7): 826–829. (in Chinese)
- [14] LEE D, BACKOFEN W A. An experimental determination of the yield locus for titanium and titanium alloy sheet[J]. *Transactions of the Metallurgical Society of AIME*, 1966, 236: 1077–1084.
- [15] SONG J H, HUH H, KIM S H. Stress-based springback reduction of a channel shaped auto-body part with high-strength steel using response surface methodology[J]. *Journal of Engineering Materials and Technology*, 2007, 129(3): 397–406.
- [16] WEI Dong-lai, CUI Zhen-shan, CHEN Jun. Optimization and tolerance prediction of sheet metal forming process using response surface model[J]. *Computational Materials Science*, 2008, 42(2): 228–233.
- [17] LIU J M, CHENA I G, CHOU T S, CHOU S S. On the deformation texture of square-shaped deep-drawing commercially pure Ti sheet[J]. *Materials Chemistry and Physics*, 2002, 77(3): 765–772.
- [18] CAO J. Reconfigurable tooling for flexible fabrication [R]. Illinois: Northwestern University, 1995.
- [19] BABA A, TOZAWA Y. Effect of tensile force in stretch-forming process on the springback[J]. *Bulletin of the Japan Society Mechanical Engineers*, 1964, 7(28): 835–843.
- [20] PARRIS A. Precision stretch forming of metal for precision assembly[D]. Cambridge: Massachusetts Institute of Technology, 1996: 126–188.

(Edited by LI Xiang-qun)